



PERGAMON

Available online at www.sciencedirect.com

SCIENCE @ DIRECT®

Polyhedron 22 (2003) 1789–1793



POLYHEDRON

www.elsevier.com/locate/poly

Ferromagnetic interactions through control of the bridging geometry

Takashi Kajiwara*, Asako Kamiyama, Tasuku Ito

Department of Chemistry, Graduate School of Science, Tohoku University, Sendai 980-8578, Japan

Received 6 October 2002; accepted 1 November 2002

Abstract

A novel trinuclear Ni(II)–Cu(II)–Ni(II) complex (**3**) and three Cu(II)–Cu(II) (**4**), Ni(II)–Cu(II) (**5**), and Mn(II)–Cu(II) (**6**) alternating chain complexes were synthesized using the complexed ligand [Cu(bptap)₂] (**1**) which acts as a bis-*mer*-tridentate ligand (bptap[−] = 2,4-bis(2-pyridyl)-1,3,5-triazapentanedienate). In all complexes, two adjoining metal ions are connected by bptap[−] in a $\kappa^2N:\kappa^3N$ bridging fashion with local C₂ symmetry. The bridging geometry forces the two d σ orbitals directed towards the ligating atoms to orthogonal to each other. Ferromagnetic interaction occurs between Cu(II)–Cu(II), Cu(II)–Ni(II), and Cu(II)–Mn(II) due to the orthogonality of the magnetic orbitals with the magnitudes of $J = 1.1 \text{ cm}^{-1}$ for **3** ($H = -2J(S_{\text{Ni}1} \cdot S_{\text{Cu}} + S_{\text{Cu}} \cdot S_{\text{Ni}2})$), $J = 1.4 \text{ cm}^{-1}$ for **4** ($H = -2J\sum_i S_{\text{Cu}i} S_{\text{Cu}i+1}$), and $\theta = 7.5 \text{ K}$ for **5** and 1.1 K for **6** (Curie–Weiss model), respectively.

© 2003 Elsevier Science Ltd. All rights reserved.

Keywords: Complexed ligand; $\kappa^2N:\kappa^3N$ Bridging fashion; Local C₂ symmetry; Ferromagnetic behavior

1. Introduction

The chemistry of multi-metal-centered complexes or metal complex assemblies involving ferromagnetic interactions has attracted much attention [1]. In such chemistry, the ‘metal containing ligands’ can facilitate the formation of the multi-metal structures and can help to control the magnetic interactions between the metal ions. Several mechanisms have been proposed to produce ferromagnetic interactions between metal centers [2] such as magnetic orbital orthogonality [3], spin polarization [4], double exchange [5], and so on. The orbital orthogonality can be introduced carefully by designing the bridging geometry of the ligand. Our strategy in the synthesis of multimetal complexes is to employ a complexed ligand [6–9] in which the bridging sites have a geometry to force the two d σ orbitals to orthogonal and to mediate a ferromagnetic interaction in several combinations of transition metal ions. Re-

cently, we reported a novel monocopper(II) complex, [Cu(bptap)₂] (**1**), which acts as a bis-tridentate bridging ligand (bptap[−] = 2,4-bis(2-pyridyl)-1,3,5-triazapentanedienate) [6].

The bptap[−] moiety in **1** acts as a pentaaza ligand with a peculiar bridging geometry of $\kappa^2N:\kappa^3N$ mode and has local C₂ symmetry. As a result, the two d_{x²−y²} orbitals of adjoining copper(II) ions are orthogonally arranged causing ferromagnetic coupling in the tricopper(II) complex *catena*-[Cu₃(bptap)₂(OAc)₂](ClO₄)₂ (**2**) (Fig. 1) with **1** as a bis-tridentate ligand. Similar orthogonality is expected between the d σ spin of the Cu(II) ion in **1** and d σ spin(s) of Cu(II), Ni(II), and Mn(II) ions in the O_h formalism, respectively.

In this report, a mixed metal trinuclear complex [$\{\text{Ni}(\text{paphy})\}_2(\mathbf{1})\}(\text{PF}_6)_4$ (**3**) (paphy = pyridine-2-aldehyde 2′-pyridylhydrazone) and three alternate chain complexes composed of **1** and Cu(II), Ni(II), and Mn(II) ions, *catena*-[Cu(**1**)](NO₃)₂ (**4**), *catena*-[Ni(**1**)](ClO₄)₂ (**5**), and *catena*-[Mn(**1**)](NO₃)₂ (**6**), are presented. All of these complexes show ferromagnetic behavior between the metal ion pairs (Cu(II)/Cu(II), Cu(II)/Ni(II), and Cu(II)/Mn(II)) through bptap[−].

* Corresponding author. Tel.: +81-22-217-6546; fax: +81-22-217-6548.

E-mail address: kajiwara@agnus.chem.tohoku.ac.jp (T. Kajiwara).

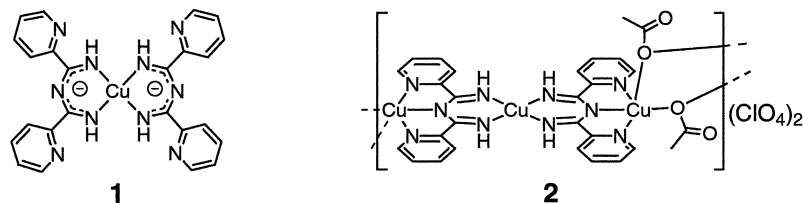


Fig. 1. The structures of the complexed ligand $[\text{Cu}(\text{bptap})_2]$ (**1**) and the tricopper(II) complex, *catena*- $[\text{Cu}_3(\text{bptap})_2(\text{OAc})_2](\text{ClO}_4)_2$ (**2**).

2. Experimental

2.1. Materials and measurements

All solvents and chemicals were purchased as reagent grade and used without further purification. $[\text{Cu}(\text{bptap})_2]$ (**1**) [6] and $[\text{NiCl}_2(\text{paphy})]$ [11] were prepared as described previously. Fourier transform infrared spectroscopy was performed on a JASCO FT/IR-620 instrument as KBr pellets. Variable-temperature magnetic susceptibility measurements were made using a SQUID magnetometer MPMS 5S (Quantum Design) at 0.5 T field. Diamagnetic correction for each sample was determined from Pascal's constants.

2.2. Preparation of complexes

2.2.1. $[\{\text{Ni}(\text{paphy})\}_2(\text{I})](\text{PF}_6)_4$ (**3**)

A solution of **1** (10 mg, 0.02 mmol) in chloroform (4 cm³) was added to a solution of $[\text{NiCl}_2(\text{paphy})]$ (13 mg, 0.04 mmol) in methanol (2 cm³). To the resulting orange solution, a solution of NH_4PF_6 (13 mg, 0.08 mmol) in methanol (0.8 cm³) was added. A yellow precipitate was obtained immediately, which was filtered and dried in the air (22.3 mg, 69%). Found: C, 34.23; H, 3.30; N, 15.17. Calc. for $\text{Ni}_2\text{CuC}_{48}\text{H}_{48}\text{N}_{18}\text{O}_2\text{P}_4\text{F}_{24}$ (**3**·2MeOH): C, 34.53; H, 2.90; N, 15.10%. IR (cm⁻¹): $\nu(\text{CN}_{\text{bptap}})$ 1616 (s), $\nu(\text{CN}_{\text{paphy}})$ 1613 (sh), $\nu(\text{PF}_6^-)$ 842 (s).

2.2.2. *catena*- $[\text{Cu}(\text{I})](\text{NO}_3)_2$ (**4**)

A solution of **1** (10 mg, 0.02 mmol) in chloroform (4 cm³) was added to a solution of $\text{Cu}(\text{NO}_3)_2 \cdot 3\text{H}_2\text{O}$ (4.8 mg, 0.02 mmol) in methanol (2 cm³). A yellow precipitate was obtained immediately, which was filtered and dried in the air (14.7 mg, 95%). Found: C, 36.70; H, 3.53; N, 21.63. Calc. for $\text{Cu}_2\text{C}_{24}\text{H}_{29}\text{N}_{12}\text{O}_{10.5}$ (**4**·4.5H₂O): C, 36.93; H, 3.74; N, 21.53%. IR (cm⁻¹): $\nu(\text{CN})$ 1612 (s), $\nu(\text{NO}_3^-)$ 1351 (s).

2.2.3. *catena*- $[\text{Ni}(\text{I})](\text{ClO}_4)_2$ (**5**)

A solution of **1** (10 mg, 0.02 mmol) in chloroform (4 cm³) was added to a solution of $\text{Ni}(\text{ClO}_4)_2 \cdot 6\text{H}_2\text{O}$ (7.3 mg, 0.02 mmol) in methanol (2 cm³). A pale orange precipitate was obtained immediately, which was filtered and dried in the air (15.5 mg, 95%). Found: C, 33.40; H, 3.00; N, 15.95. Calc. for $\text{NiCuC}_{24.5}\text{H}_{26.5}\text{N}_{10}\text{O}_{11}\text{Cl}_{3.5}$ (**5**·

$3\text{H}_2\text{O} \cdot 0.5\text{CHCl}_3$): C, 33.31; H, 3.02; N, 15.86%. IR (cm⁻¹): $\nu(\text{CN})$ 1616 (s), $\nu(\text{ClO}_4^-)$ 1091 (s).

2.2.4. *catena*- $[\text{Mn}(\text{I})](\text{NO}_3)_2$ (**6**)

A solution of **1** (10 mg, 0.02 mmol) in chloroform (4 cm³) was added to a solution of $\text{Mn}(\text{NO}_3)_2 \cdot 6\text{H}_2\text{O}$ (5.7 mg, 0.02 mmol) in methanol (2 cm³). A pale orange precipitate was obtained immediately, which was filtered and dried in the air (13 mg, 95%). Found: C, 37.16; H, 3.43; N, 21.66. Calc. for $\text{MnCuC}_{24}\text{H}_{29}\text{N}_{12}\text{O}_{10.5}$ (**6**·4.5H₂O): C, 37.34; H, 3.79; N, 21.77%. IR (cm⁻¹): $\nu(\text{CN})$ 1610 (s), $\nu(\text{NO}_3^-)$ 1349 (s).

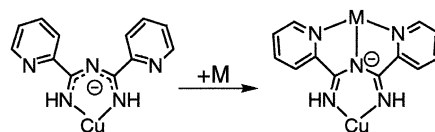
3. Results and discussion

3.1. Structures of the complexes

Although crystals of **3**–**6** could not be obtained, we can discuss the structures of these complexes with the aid of spectral data. The analytical composition for each compound is acceptable for trinuclear **3** and alternating **4**–**6**, respectively. The IR spectrum of **1** changes when it coordinates to other metal ions, reflecting a change of the electronic structure of **1** shown in Scheme 1 [6].

In **1**, the negative charge of bptap^- is delocalized over the N–C–N–C–N moiety and the double bond character of ligating –C=NH group is diminished (C–N = 1.305(3)–1.314(3) Å; $\nu(\text{CN}) = 1574 \text{ cm}^{-1}$). Upon forming the tricopper(II) complex **2**, the negative charge is trapped on the central nitrogen of the N–C–N–C–N moiety to form coordination bond with the second Cu(II) ion, and as a result, the double bond character of –C=NH is increased (C–N = 1.279(5) Å and 1.281(5) Å; $\nu(\text{CN}) = 1631 \text{ cm}^{-1}$). For **3**–**6**, the NC stretching peak for bptap^- was observed in the range of 1610–1616 cm⁻¹ suggesting that both of the N₃ sites in **1** are coordinated to metal ions.

The structure of bptap^- is very close to the di-keto ligand bpca^- (Hbpca = bis(2-pyridylcarbonyl)amine) of



Scheme 1.

which the crystal structures of mononuclear complexes involving almost all the first-row transition metal ions have been reported [12]. In all complexes, bpca^- acts as a *mer*- N_3 ligand coordinating in a manner similar to terpyridine, and it is expected that the each N_3 site in **1** coordinates to metal ion in the tridentate *mer*-fashion. For **3**, two CN stretching bands were observed at 1616 and 1613 cm^{-1} . The latter is similar to $[\text{Ni}(\text{paphy})\text{Cl}_2]$ in which the paphy ligand coordinates to Ni(II) ion in a *mer*-manner. The spectral data suggest that the coordination of paphy is unchanged and the structure of **3** can be depicted as Fig. 2.

For **4–6**, the structures of insoluble products are inferred as alternating one-dimensional chain polymers shown in Fig. 3 which agrees with the analytical composition.

In these compounds, the coordination sites of the second metal ions M are occupied by six nitrogen atoms from two complexed ligands in a tridentate *mer*-fashion, being similar to $[\text{Cu}(\text{bpca})_2]$, $[\text{Ni}(\text{bpca})_2]$, and $[\text{Mn}(\text{bpca})_2]$, respectively. The IR signals for the counter anions (NO_3^- for **4** and **6** and ClO_4^- for **5**, respectively) indicate that they are free from coordination in spite of their coordination abilities, and this also suggests that the coordination around M is completed by the nitrogen donor sets from two complexed ligands **1**.

3.2. Magnetic properties

Temperature dependent magnetic susceptibilities of complexes **3–6** were measured down to 2.0 K shown in Figs. 4–7, respectively. The temperature dependence of χ_M^{-1} for chain complexes **5** and **6** are shown as insets in Figs. 6 and 7. The susceptibility value for complex **3** was calculated for three spin centers, whereas the values for the one-dimensional **4–6** were calculated for repeating units including two adjoining metal ions. In all complexes, the $\chi_M T$ value increases as the temperature is lowered, which suggests the presence of ferromagnetic interaction between adjoining metal ions.

The $\chi_M T$ for **3** is constant with the value of approximately $2.8\text{ emu K mol}^{-1}$ down to 40 K and shows an increase on further lowering of the temperature, reaching a maximum value of $3.77\text{ emu K mol}^{-1}$ at 3 K. The values around room temperature are consistent with the spin only value for $(S_{\text{Ni1}}, S_{\text{Cu}}, S_{\text{Ni2}}) = (1, 1/2, 1)$ if an averaged g of 2.16 is used. The temperature

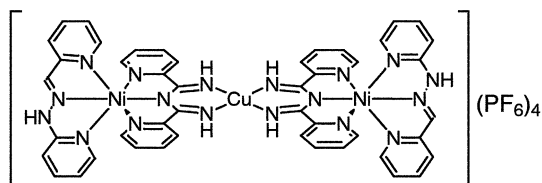


Fig. 2. The proposed structure of the trinuclear complex **3**.

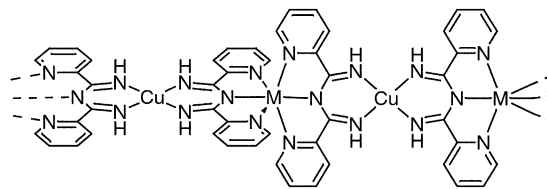


Fig. 3. The proposed structure of cationic part of chain complexes **4–6** ($M = \text{Cu(II)}$ for **4**, Ni(II) for **5**, and Mn(II) for **6**).

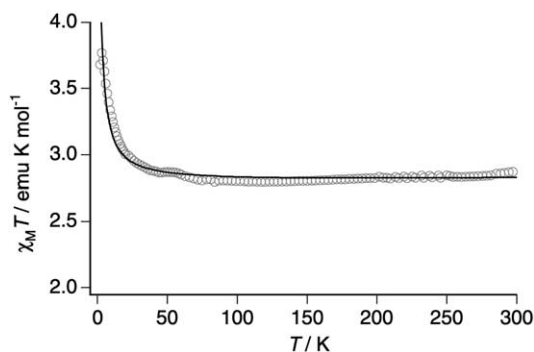


Fig. 4. The temperature dependence of $\chi_M T$ for **3**. The solid line is the theoretical curve for which parameters are given in the text.

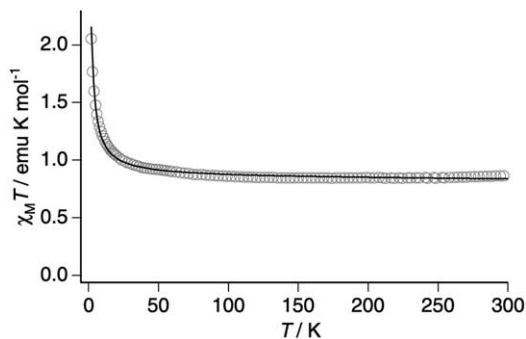


Fig. 5. The temperature dependence of $\chi_M T$ for **4**. The solid line is the theoretical curve based on the Heisenberg chain expression for which parameters are given in the text.

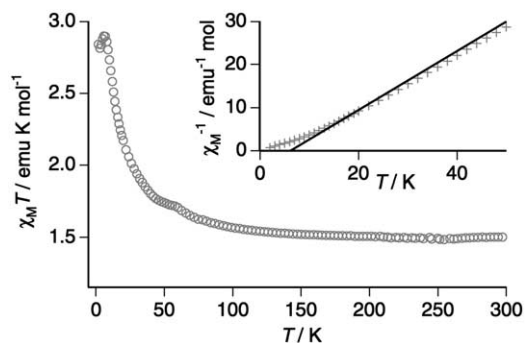


Fig. 6. The temperature dependence of $\chi_M T$ for **5**. The inset shows a plot of χ_M^{-1} vs. T , in which the solid line corresponds to the theoretical line based on the Curie–Weiss model.

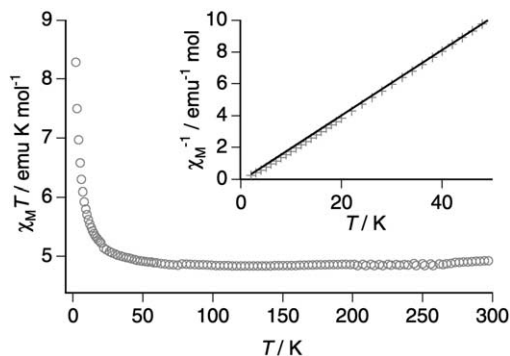


Fig. 7. The temperature dependence of $\chi_M T$ for **6**. The inset shows a plot of χ_M^{-1} vs. T , in which the solid line corresponds to the theoretical line based on the Curie–Weiss model.

dependence of $\chi_M T$ was analyzed by an isolated three-spin model ($H = -2J(S_{\text{Ni1}} \cdot S_{\text{Cu}} + S_{\text{Cu}} \cdot S_{\text{Ni2}})$) [2]. The best fit parameter was estimated as $J = 1.1(1) \text{ cm}^{-1}$ with an averaged g value of 2.16(1).

The $\chi_M T$ value for **4** at room temperature, $0.86 \text{ emu K mol}^{-1}$, is slightly larger than the expected spin only value for two Cu(II) ions, $0.75 \text{ emu K mol}^{-1}$. The $\chi_M T$ value is almost constant down to 50 K and it shows abrupt increase at lower temperatures. The temperature dependence of the $\chi_M T$ value for **4** was analyzed by a Heisenberg model,

$$\chi T = \frac{N\beta^2 g^2}{4k} \times 2 \times \left[\frac{N}{D} \right]^{\frac{2}{3}}$$

where $D = 1 + 2.798x + 7.009x^2 + 8.654x^3 + 4.574x^4$,

$N = 1 + 5.798x + 16.903x^2 + 29.377x^3 + 29.833x^4 + 14.037x^5$,

and $x = \frac{J}{kT}$

with the Hamiltonian $H = -2J\sum_i S_{\text{Cu}i} \cdot S_{\text{Cu}i+1}$ [2]. The J value was estimated to be $2.8(1) \text{ cm}^{-1}$ with a g value of 2.13.

For **5**, the $\chi_M T$ value at 300 K, $1.50 \text{ emu K mol}^{-1}$, is slightly larger than the spin only value of $1.38 \text{ emu K mol}^{-1}$ expected for the dilute two magnetic centers (Ni(II) with $S = 1$ and Cu(II) with $S = 1/2$) with an average g value of 2.00. On lowering the temperature, the $\chi_M T$ value gradually increases down to 50 K, and below 30 K, it increases rapidly to reach the maximum value of $2.90 \text{ emu K mol}^{-1}$ at 6 K. The decrease of $\chi_M T$ value at lower temperature is mainly due to the zero-field splitting of Ni(II) ions. The magnitude of the interaction was estimated in the temperature range of 20–300 K as $\theta = 7.5(2) \text{ K}$ on the basis of the Curie–Weiss model. The $\chi_M T$ value for **6** at 300 K, $4.92 \text{ emu K mol}^{-1}$, is slightly larger than the sum of the spin only

values of 0.375 and $4.370 \text{ emu K mol}^{-1}$ for the two spin carriers (Cu(II) with $S = 1/2$ and Mn(II) with $S = 5/2$) with an average g value of 2.00, which is almost constant down to 50 K. Below 20 K, it increase rapidly to reach $8.29 \text{ emu K mol}^{-1}$ at 2 K. The magnetic behavior was analyzed by the Curie–Weiss model in the temperature range of 20–250 K to give the value of $\theta = 1.0(1) \text{ K}$.

As we expected, ferromagnetic coupling was observed in all of the multinuclear complexes, and the propagation of the ferromagnetic interaction can be understood by the spin orbital orthogonality which is similar to the VO(d_{xy})–Cu($d_{x^2-y^2}$) system [3]. In the complexes, the magnetic interactions are mediated by bptap^- which bridges Cu(II) and metal ion M (Ni(II) for **3** and **5**, Cu(II) for **4**, and Mn(II) for **6**) in a $\kappa^2 N : \kappa^3 N$ mode with local C_2 symmetry along the Cu–M axis. The Cu(II) ion has a $d\sigma$ spin in the $d_{x^2-y^2}$ orbital directed towards the donor N-atoms from the bridging ligand. As well, both Ni(II) and Mn(II) ions have two $d\sigma$ spins in the $d_{x^2-y^2}$ and d_{z^2} orbitals in the O_h formalism both directed towards the N_3 donor set from bptap^- (Fig. 8).

Two different configurations of magnetic orbitals are expected depending on the coordination formalisms around M. However, two neighboring magnetic orbitals in both cases have different symmetry about a twofold rotation axis, i.e. the $\text{Cu}_{\text{central}}$ is antisymmetric whereas the M is symmetric, and hence the magnetic orbitals in each pair are orthogonal to each other. This orthogonality is advantageous to ferromagnetic coupling.

The ferromagnetic interaction in **4** is weaker than in **2** for which the J value has been estimated as 7.5 cm^{-1} [6]. The different strength of the interaction between **2** and **4** might be due to the differences in coordination environments around the Cu(II) ions in the N_3 sites. In **2**, the magnetic orbitals of Cu(II) ions are coplanar and directly connected by the N–C–N–C–N moiety of the bptap^- ligand (Fig. 8(a)). In **4**, it is expected that the Cu(II) ion in the N_3 site is in a slightly distorted octahedral environment as found in $[\text{Cu}(\text{bpca})_2]$ [12a]. The two e_g orbitals of this site exist in different arrangements: one is perpendicular to and the other is coplanar with the Cu(II) ion in **1** (Fig. 8(b) left and right, respectively). In the former case, the two magnetic orbitals are not directly connected by the N–C–N–C–N moiety and the contribution of this configuration diminishes the interaction in **4** compared with **2**.

$J = 1.1 \text{ cm}^{-1}$ for **3** and $\theta = 7.5 \text{ K}$ (5.2 cm^{-1}) for **5** are roughly consistent, taking into consideration that θ is correlated to zJ' in the molecular field approximation [2].

The magnetic interaction in **6** is much weaker than those for the Cu(II)/Cu(II) and Cu(II)/Ni(II) systems. As it found in $[\text{Mn}(\text{bpca})_2]$, the averaged Mn–N distance is longer than the averaged Ni–N and Cu–N distances in $[\text{Ni}(\text{bpca})_2]$ and $[\text{Cu}(\text{bpca})_2]$ [12], and this

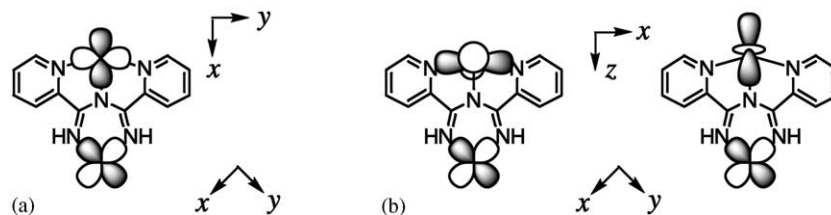


Fig. 8.

feature is mainly reflected in the weaker ferromagnetic interaction. As well, the Mn(II) ion in **6** has both $d\pi$ spins in t_{2g} orbitals and $d\sigma$ spins in e_g orbitals in the O_h formalism, in contrast to the Cu(II) and Ni(II) ions in **4** and **5**. The t_{2g} orbitals of Mn(II) and the e_g orbital of Cu(II) ion in **1** have the same symmetry with respect to the rotation around the twofold axis superimposed on the Mn–Cu axis and have a non-zero overlap integral. The non-zero overlap integral causes antiferromagnetic coupling as we reported for a high-spin Fe(II)/Cr(III) system [10]. This overlap also makes the ferromagnetic interaction weaker in **6**.

4. Conclusions

In this study, we have reported the syntheses and the magnetic behavior of a trinuclear complex and one-dimensional complexes involving an alternating arrangement of the complexed ligand **1** and divalent copper, nickel, and manganese ions. All of the complexes have ferromagnetic interaction due to the bridging geometry controlled by the $bptap^-$ ligand. Orthogonality is generally expected for all combinations of metal ions containing $d\sigma$ spin(s), and we have shown that the complexed ligand **1** is a useful ferromagnetic coupler.

Acknowledgements

This work was supported by Grant-in-Aid for Scientific Research on Priority Areas (No. 10149102) and by Encouragement of Young Scientists (No. 13740370) from the Ministry of Education, Culture, Sports, Science, and Technology, Japan, as well as by JSPS

Research Fellowships for Young Scientists (No. 12006281).

References

- [1] (a) H.O. Stumpf, L. Ouahab, Y. Pei, D. Grandjean, O. Kahn, *Science* 261 (1993) 447;
(b) S.L. Suib, *Chem. Rev.* 93 (1993) 803.
- [2] O. Kahn, *Molecular Magnetism*, VCH, New York, 1993.
- [3] (a) J.B. Goodenough, *Phys. Rev.* 100 (1955) 564;
(b) J. Kanamori, *J. Phys. Chem. Solids* 10 (1959) 87;
(c) O. Kahn, J. Galy, Y. Journaux, J. Jaid, I. Morgenstern-Badarau, *J. Am. Chem. Soc.* 104 (1982) 2165;
(d) N. Torihara, H. Okawa, S. Kida, *Chem. Lett.* (1978) 1269.
- [4] (a) I. Fernández, R. Ruiz, J. Faus, M. Julve, F. Lloret, J. Cano, X. Ottenwaelder, Y. Journaux, M.C. Muñoz, *Angew. Chem., Int. Ed.* 40 (2001) 3039;
(b) F. Lloret, G. de Munno, M. Julve, J. Cano, R. Ruiz, A. Caneschi, *Angew. Chem., Int. Ed.* 37 (1998) 135;
(c) H. Oshio, H. Ichida, *J. Phys. Chem.* 99 (1995) 3294.
- [5] (a) C. Zener, *Phys. Rev.* 82 (1951) 403;
(b) P.W. Anderson, H. Hasegawa, *Phys. Rev.* 100 (1955) 675;
(c) G. Blondin, J.-J. Girerd, *Chem. Rev.* 90 (1990) 1359.
- [6] T. Kajiwara, A. Kamiyama, T. Ito, *Chem. Commun.* (2002) 1256.
- [7] A. Kamiyama, T. Noguchi, T. Kajiwara, T. Ito, *Inorg. Chem.* 41 (2002) 507.
- [8] T. Kajiwara, T. Ito, *J. Chem. Soc., Dalton Trans.* (1998) 3351.
- [9] A. Kamiyama, T. Noguchi, T. Kajiwara, T. Ito, *Angew. Chem., Int. Ed.* 39 (2000) 3130.
- [10] T. Kajiwara, R. Sensui, T. Noguchi, A. Kamiyama, T. Ito, *Inorg. Chim. Acta* 337 (2002) 299.
- [11] F. Lions, I.G. Dance, J. Lewis, *J. Chem. Soc. (A)* (1967) 565.
- [12] (a) D. Marcos, R. Martínez-Mañez, J.-V. Folgado, A. Beltrán-Porter, D. Beltrán-Porter, A. Fuertes, *Inorg. Chim. Acta* 159 (1989) 11;
(b) D. Marcos, J.-V. Folgado, D. Beltrán-Porter, M.T. do Prado-Gambardella, S.H. Pulcinelli, R.H. de Almeida-Santos, *Polyhedron* 9 (1990) 2699;
(c) S. Wocadlo, W. Massa, J.-V. Folgado, *Inorg. Chim. Acta* 207 (1993) 199.